

A Kv7.2 mutation associated with early onset epileptic encephalopathy with suppression-burst enhances Kv7/M channel activity

*Jérôme Devaux, ††Affef Abidi, §¶Agathe Roubertie, #**Florence Molinari, #**Hélène Becq, ††††Caroline Lacoste, ††Laurent Villard, ††††Mathieu Milh, and #**Laurent Aniksztejn

SUMMARY

Mutations in the *KCNQ2* gene encoding the voltage-gated potassium channel subunit Kv7.2 cause early onset epileptic encephalopathy (EOEE). Most mutations have been shown to induce a loss of function or to affect the subcellular distribution of Kv7 channels in neurons. Herein, we investigated functional consequences and subcellular distribution of the p.V175L mutation of Kv7.2 (Kv7.2^{V175L}) found in a patient presenting EOEE. We observed that the mutation produced a 25–40 mV hyperpolarizing shift of the conductance–voltage relationship of both the homomeric Kv7.2^{V175L} and heteromeric Kv7.2^{V175L}/Kv7.3 channels compared to wild-type channels and a 10 mV hyperpolarizing shift of Kv7.2^{V175L}/Kv7.2/Kv7.3 channels in a 1:1:2 ratio mimicking the patient situation. Mutant channels also displayed faster activation kinetics and an increased current density that was prevented by 1 μM linopirdine. The p.V175L mutation did not affect the protein expression of Kv7 channels and its localization at the axon initial segment. We conclude that p.V175L is a gain of function mutation. This confirms previous observations showing that mutations having opposite consequences on M channels can produce EOEE. These findings alert us that drugs aiming to increase Kv7 channel activity might have adverse effects in EOEE in the case of gain-of-function variants.

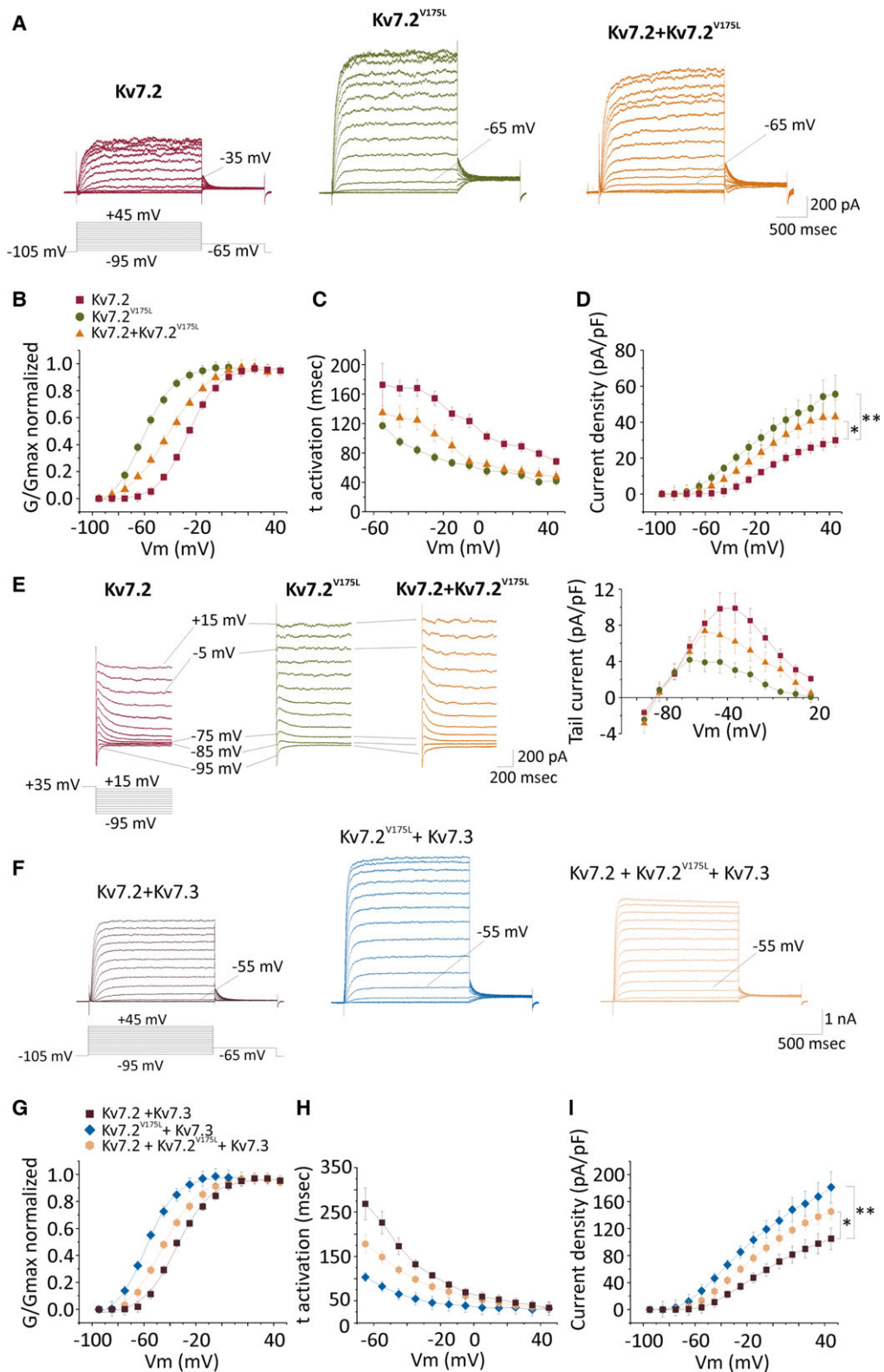
KEY WORDS: Early onset epileptic encephalopathy, *KCNQ2*, M-current, Gain of function, Axon initial segment, Linopirdine.

De novo mutations in *KCNQ2* have been identified in patients with early onset epileptic encephalopathy (EOEE).¹ *KCNQ2* encodes the Kv7.2 protein and forms homomeric

or, in association with Kv7.3, heteromeric voltage-gated potassium channels responsible for the M current.^{1,2} These channels are expressed at high density at the axon initial segment (AIS) and at the nodes of Ranvier, where they regulate neuronal firing.^{3–5} Each Kv7 subunit consists of intracellular N- and C-terminal domains and six transmembrane segments forming the voltage-sensing (S1–S4) and the pore (S5–P–S6) domains. Functional analysis of EOEE mutations in heterologous cells showed variable effects on the M current. All mutations located within the S5–S6 or the C-terminal domains decrease M-current amplitude from a moderate (~25%) to a strong (>50%) level.^{6,7} However, three reported mutations located in the S2 (p.R144Q) and S4 (p.R201C and p.R201H) regions of Kv7.2 actually increased M-current amplitude.⁸ This suggested that EOEE mutations located in the voltage-sensing domain can be gain of function mutations. We recently identified the mutation

*CNRS, Aix-Marseille University, CRN2M-UMR7286, Marseille, France; †GMGF, Aix-Marseille University, Marseille, France; ‡INSERM, UMR_S 910, Marseille, France; §Pediatric Neurology Department, Montpellier University Hospital, Montpellier, France; ¶INSERM U1051, INM Montpellier, Montpellier, France; #Mediterranean Neurobiology Institute INMED, Aix-Marseille University, Marseille, France; **INSERM, UMR_S 901, Marseille, France; and ††Timone Children Hospital, Pediatric Neurology Department, APHM, Marseille, France

Address correspondence to Laurent Aniksztejn, INMED-INSERM U901, parc Scientifique de Luminy, 13273 Marseille Cedex 09, France. E-mail: laurent.aniksztejn@inserm.fr and Mathieu Milh, Hôpital d'Enfants de la Timone, Service de neurologie pédiatrique, APHM, rue St Pierre, 13005 Marseille, France. E-mail: mathieu.milh@ap-hm.fr



p.V175L located in S3 region of Kv7.2 in a patient with EOEE.⁹ Herein we show that this mutation increases M-channel activity and does not affect channel distribution in neurons.

METHODS

The experimental procedures and data analysis used in the present study have been described previously.⁷

RESULTS

Clinical features of the patient carrying the p.V175L mutation

The female patient was born from healthy, nonconsanguineous parents. During pregnancy, there was a fetal growth restriction associated with hip displacement. Fetal karyotype was normal. The patient was born at 34 post-conceptional weeks. At birth, the weight was 2,040 g, the height was 44 cm, and the cranial circumference was 30 cm. The first neurologic examination was abnormal with no arousal, no eye contact, and axial hypotonia. The patient had a cleft palate and she became hypertonic with pyramidal signs and global spasticity. Electroencephalography (EEG) performed during the first day of life showed a suppression-burst pattern with periods of silence longer than those of burst (Fig. S1). The bursts of activity were initially asymptomatic. Epilepsy began during the second week of life with frequent erratic and axial myoclonic jerks. EEG still showed a suppression-burst pattern and symptomatic bursts of activity associated with myoclonic jerks that lasted longer than the periods of silence. There were no spasms or clonic seizure, only erratic and massive myoclonic jerks. Pyridoxine and pyridoxal phosphate trials were ineffective, as was phenobarbital, vigabatrin, and topiramate. Brain magnetic resonance imaging (MRI) performed at day 13 did not show any brain malformation. Metabolic screening and comparative genomic hybridization (CGH) were normal. Psychomotor achievements were limited and progressive spastic tetraparesis was observed. The patient needed gastrostomy feeding due to swallowing difficulties. The patient died at 18 months (probable sudden unexpected death in epilepsy [SUDEP]).

Functional consequences of p.V175L mutation

We investigated the electrophysiologic consequences of the p.V175L mutation on homomeric Kv7.2 channels and

heteromeric Kv7.2/Kv7.3 channels expressed in Chinese hamster ovary (CHO) cells. Homomeric Kv7.2 wild-type channels generated a slowly activating outward current in response to depolarizing voltage steps from a holding potential of -105 mV with a threshold potential of around -45 mV. The $V_{1/2}$ and K slope values were -25 ± 1.9 mV and 12.7 ± 1.04 mV/e-fold, respectively ($n = 10$ cells; Fig. 1A,B). The p.V175L mutation strongly affected the gating properties of the channel. We observed a large hyperpolarizing shift in the conductance/voltage (G/V) relationship of Kv7.2^{V175L} channels. The threshold potential of Kv7.2^{V175L} channels was around -75 mV with a $V_{1/2}$ value of -62.3 ± 1.09 mV ($n = 13$ cells, $p < 10^{-6}$, analysis of variance [ANOVA] followed by Bonferroni test), and a K slope factor of 13.05 ± 0.89 mV/efold (not significant) (Fig. 1B). The current density was increased by 90% (measured at $+45$ mV), and the activation time constant was also twice faster at all membrane potentials (Fig. 1C,D). Because of the negative shift, there were fewer channels that deactivate during hyperpolarizing voltage steps applied from $+35$ mV compared to wild-type channels; consequently tail currents of mutant channels had lower amplitude (Fig. 1E). Tail currents from both channels reversed polarity at the same membrane potential (~ -88 mV, Fig. 1E), a value close to the equilibrium potential of K^+ in our recording condition.⁷ This indicated that the p.V175L mutation did not affect the ionic selectivity of the channels. Deactivation channel kinetics were also not significantly affected by the mutation at all potentials tested (data not shown). The co-transfection of Kv7.2 with Kv7.2^{V175L} in a 1:1 ratio attenuated but did not abolish the impact of the mutation on channel gating. The negative shift of the G/V relationship was reduced to 10 mV, but the $V_{1/2}$ was significantly different from wild-type channels (-40.4 ± 2.9 mV; $n = 8$, $p < 10^{-4}$). The activation time constant was also significantly faster and the current density was significantly increased (by 45% at $+45$ mV, Fig. 1B–D).

Figure 1.

Electrophysiologic consequences of the p.V175L mutation on homomeric and heteromeric channels. **(A)** Current evoked by 10 mV incremental depolarizing voltage steps from -105 mV to $+45$ mV for 2 s followed by a 1 s hyperpolarizing voltage step to -65 mV in CHO cells transfected with wild-type Kv7.2 (left), Kv7.2^{V175L} (middle), or Kv7.2^{V175L}/Kv7.2 (right). **(B)** Conductance–voltage relationship of homomeric Kv7.2 channels (red squares), Kv7.2^{V175L} (green circles), and Kv7.2^{V175L}/Kv7.2 (orange triangles) each normalized to their maximal conductance. Continuous lines represent Boltzmann fits to the experimental data. **(C)** Activation time constant plotted as a function of the membrane potential (V_m). **(D)** Current densities are represented as a function of V_m . Plotted data in **A–D** are from currents evoked by 19, 25, and 14 series of incremental depolarizing voltage steps performed in cells expressing Kv7.2 ($n = 10$ cells), Kv7.2^{V175L} ($n = 13$ cells), and Kv7.2/Kv7.2^{V175L} ($n = 8$ cells), respectively. **(E)** Tail currents observed after a 1 s hyperpolarizing voltage steps from $+35$ mV to potentials ranging from $+15$ mV to -95 mV. Amplitude of each currents was measured and plotted as a function of V_m . The data are from currents evoked by 10, 11, and 6 series of hyperpolarizing voltage steps performed in cells expressing Kv7.2 ($n = 10$ cells), Kv7.2^{V175L} ($n = 11$ cells), and Kv7.2/Kv7.2^{V175L} ($n = 6$ cells), respectively. **(F–I)** Same as **A–D** for heteromeric channels Kv7.2/Kv7.3 (dark brown squares), Kv7.2^{V175L}/Kv7.3 (blue diamonds), and Kv7.2^{V175L}/Kv7.2/Kv7.3 (light orange hexagons). Plotted data are from currents evoked by 26, 21, and 24 series of incremental depolarizing voltage steps performed in cells expressing Kv7.2/Kv7.3 ($n = 14$ cells), Kv7.2^{V175L}/Kv7.3 ($n = 12$ cells), and Kv7.2^{V175L}/Kv7.2/Kv7.3Kv7.2 ($n = 14$ cells), respectively. Statistics analysis: * $p < 0.05$; ** $p < 0.01$ (ANOVA followed by Bonferroni's test).

We then analyzed the consequences of the mutant subunit associated with Kv7.3 in a 1:1 ratio (Kv7.2^{V175L}/Kv7.3) and with both Kv7.2 and Kv7.3 subunits in a 1:1:2 ratio, a configuration that is theoretically observed in patients. The mutation induced a negative shift of the G/V relationship in both configurations with significantly more hyperpolarized V_{1/2} values than that of Kv7.2/Kv7.3 channels (Fig. 1G). The V_{1/2} values (in mV) were of -33.5 ± 0.83, -59.5 ± 1.5, and -44.7 ± 1.25 for Kv7.2/Kv7.3 (n = 14), Kv7.2^{V175L}/Kv7.3 (n = 12), and Kv7.2^{V175L}/Kv7.2/Kv7.3 (n = 14) channels, respectively (*p* < 10⁻⁴, mutant channels vs. wild-type channel). The K slope factor was significantly decreased for Kv7.2^{V175L}/Kv7.3 channels only. The K values (in mV/e-fold) were 14.1 ± 0.72, 11.2 ± 0.58 (*p* < 0.01), and 14.2 ± 0.84. The activation time constants of both Kv7.2^{V175L}/Kv7.3 and Kv7.2^{V175L}/Kv7.2/Kv7.3 channels were significantly faster for currents evoked by

depolarizing voltage steps up to +15 mV and up to -15 mV, respectively, and current densities at +45 mV increased by 72% and 38% (Fig. 1H,I).

We then examined whether linopirdine, a cognitive enhancer known to inhibit M current, could restore mutant channel current density close to that of wild-type. The current density carried by Kv7.2^{V175L}/Kv7.2/Kv7.3 channels was not significantly different from that of Kv7.2/Kv7.3 channels at 1 μM of linopirdine (Fig. 2A,C). However, linopirdine did not prevent the shift of the mutant channels G/V relationship (Fig. 2D). The V_{1/2} (in mV) were -40.5 ± 1.4 (n = 13), -41.8 ± 1.3 (n = 12), and -40.9 ± 1.2 (n = 10) for 1, 3, and 10 μM of linopirdine, respectively. In contrast to linopirdine, retigabine significantly enhanced mutant channel current density and further shifted the V_{1/2} value to -75.2 ± 2.0 mV (Fig. 2C,D; n = 5). Linopirdine showed similar effects on Kv7.2/Kv7.2^{V175L} channels and restored a

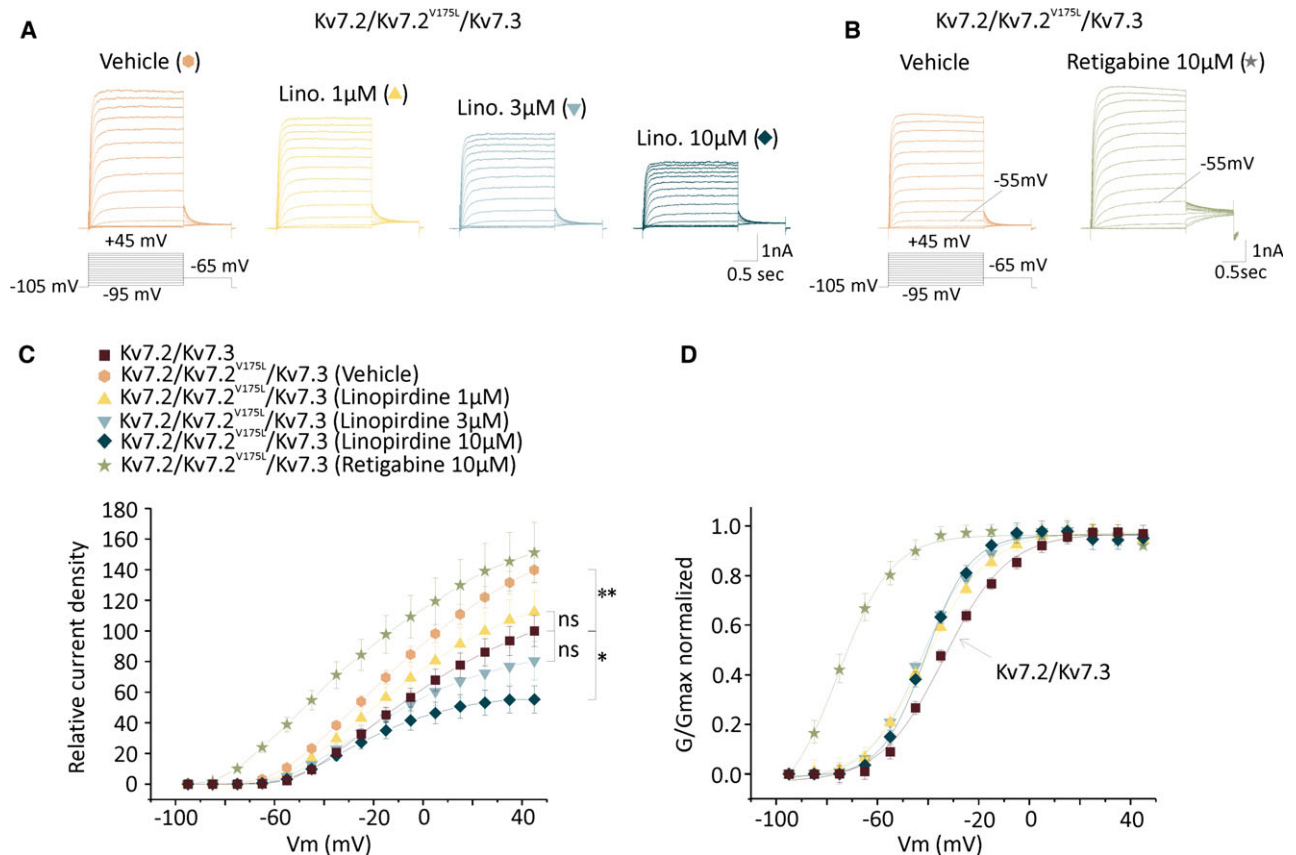


Figure 2.

Effects of linopirdine and retigabine on heteromeric mutant channels. (**A** and **B**) Currents evoked by incremental depolarizing voltage steps in the absence (vehicle) and the in presence of linopirdine at 1, 3, and 10 μM (**A**) or of retigabine 10 μM (**B**) in cells expressing Kv7.2/Kv7.2^{V175L}/Kv7.3 channels. (**C**) Relative current densities measured at all voltage steps showing the effects of linopirdine at 1 μM (yellow triangles), 3 μM (light blue triangles), and 10 μM (dark blue diamonds) or that of retigabine 10 μM (green stars) in cells expressing Kv7.2/Kv7.2^{V175L}/Kv7.3 channels. Values were normalized to the mean current density measured at +45 mV in CHO expressing wild-type Kv7.2/Kv7.3 subunits (dark brown squares). (**D**) Conductance–voltage relationship of heteromeric Kv7.2/Kv7.3 and Kv7.2/Kv7.2^{V175L}/Kv7.3 in the presence of linopirdine at 1, 3, 10 μM or retigabine 10 μM, each normalized to their maximal conductance. Continuous lines represent Boltzmann fits to the experimental data.

current density close to that of Kv7.2 channels at 1 μM (data not shown).

We then examined by western blot and biotinylation assay whether the p.V175L mutation affected the total and cell surface expression of both homomeric and heteromeric proteins (Fig. S2). The p.V175L mutation did not significantly affect the expression of the heteromeric channels, but solely increased the surface expression of the homomeric proteins.

We previously found that EOOE mutations affected the targeting of Kv7.2/Kv7.3 channels at the AIS in neurons.⁷ We examined whether the p.V175L mutation also affects the location of Kv7 channels in hippocampal neurons. We found that both wild-type Kv7.2/Kv7.3 and Kv7.2^{V175L}/Kv7.3 heteromers were expressed at the AIS and colocalized with ankyrin-G. The ratios of labeling of heteromeric channels at AIS/dendrite or AIS/soma were

not significantly different between wild-type and mutant channels (Fig. 3).

Taken together, our data suggested that the mutant protein may exert a gain of function at the AIS in the patient.

DISCUSSION

Together with a recent study,⁸ our data provide new evidence that a gain of function mutation in Kv7.2 channels can lead to EOOE. Of interest, we show here that this mutation does not impact the protein traffic, suggesting that the mutant protein may exert its pathogenic function at its proper neuronal location. The epileptic features of the patient with p.V175L mutation appeared similar to those described in patients with loss-of-function mutations in KCNQ2.^{7,10} This indicated that both types of mutations have similar deleterious consequences. It is unclear whether

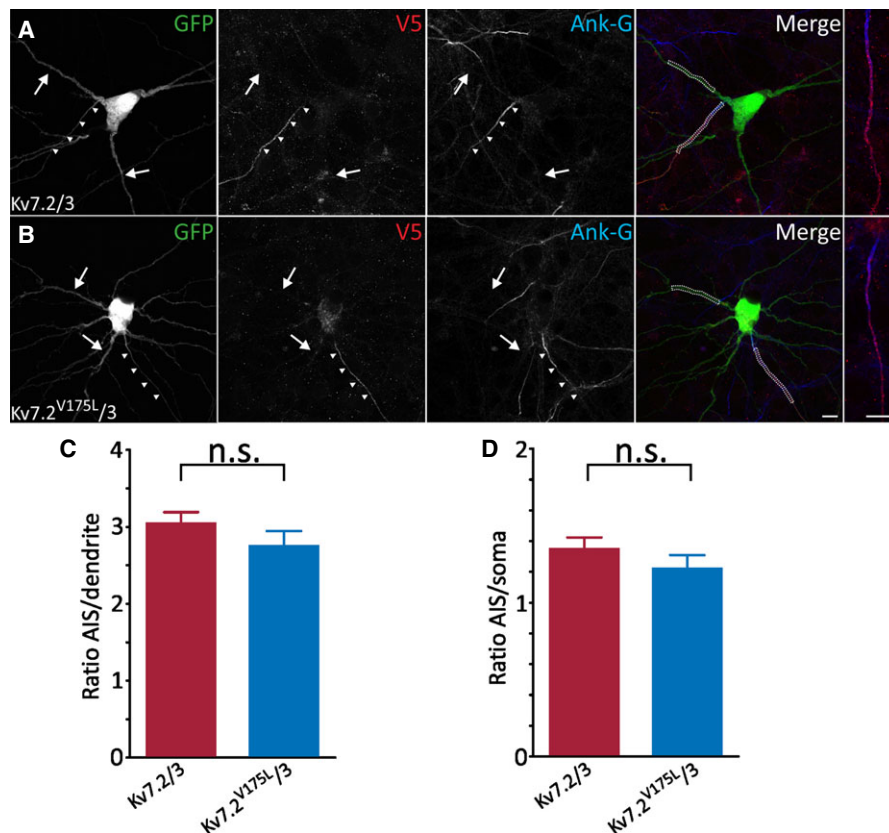


Figure 3.

The p.V175L mutation does not affect the targeting of Kv7 channels in neurons. (**A** and **B**) Cultured hippocampal neurons were transfected at 7 days in vitro with V5-tagged Kv7.2 (**A**) or V5-tagged Kv7.2^{V175L} constructs (**B**) together with hKv7.3 and enhanced green fluorescent protein (EGFP; green), and then were immunostained 2 days later for V5 (red) and ankyrin-G (blue) to label the AIS (arrowheads). Wild-type Kv7.2/Kv7.3 channels (**A**) were selectively addressed at the AIS where they co-localized with ankyrin-G, but were not detected in dendrites (arrows). The heteromeric association of wild-type Kv7.3 with the mutant Kv7.2^{V175L} subunit did not affect the localization of the channels at AIS (**B**). Isolated AIS labeling are shown at a higher magnification in the right panels. (**C** and **D**) The intensity of V5 staining was measured along a 20–30 μm long selection (dashed lines) within the AIS, dendrites, and soma, and the fluorescence ratios AIS/dendrite (**C**) and AIS/soma were calculated ($n = 20$ neurons for each condition). n.s. not significant (ANOVA followed by Bonferroni's test with multiple-comparisons). Scale bars: 10 μm .

the fetal growth restriction, cleft palate, and hip displacement are related to the mutation of *KCNQ2*, even if some fetal abnormalities have also been reported only in a patient with another gain of function mutation in *KCNQ2*.¹¹

The molecular mechanism by which the p.V175L mutation in S3 affects the gating of Kv7 channel is not known. Of interest, both p.V175L and p.R201H mutations induce similar changes in $V_{1/2}$ values in homomeric and heteromeric channels.⁸ It was suggested that the positively charged arginine residue at position 201 in S4 contracts electrostatic interactions with negatively charged residues in S2 (E140) and S3 (D172), thereby leading to the stabilization of the voltage-sensing domain at resting state.⁸ The stability of this domain is reduced by the replacement of the arginine by a histidine, which is less charged at pH 7. Both valine and leucine residues are not ionized at physiologic pH. These two residues have similar properties but differ only by their radical, leucine being a bulkier residue than valine. We thus suspect that this substitution may change the conformation of S3 and impair the electrostatic interaction between the residues in S4 and S2–S3 in a manner similar to the p.R201H mutation. In addition, we found that the p.V175L increased the surface expression of homomeric mutant channels, but not heteromeric channels with Kv7.3. This effect may contribute to the increase in current densities observed for homomeric mutant channels. Previously, we also found that p.A294V mutation affected the expression of homomeric Kv7.2 channel, but not heteromeric channels.⁷ Together, this suggests that the association with Kv7.3 is protective and may partly compensate for conformational changes and restore a normal protein sorting. However, these results were obtained in heterologous systems and may not necessarily reflect what is observed in vivo.

It is difficult to understand how the p.V175L mutation can be responsible for the epileptic disorder since in principle, at the cellular level, the mutant channel should dampen neuronal excitability. It may be, as suggested by Miceli et al.⁸ with other gain of function mutations, that interneurons are more impacted than pyramidal cells by an increase in M current, thus creating an imbalance between excitation and inhibition.

It is also unclear why both gain- and loss-of-function mutations lead to the same phenotype. One may speculate that no matter the impact on Kv7 channel activity, what is important is that these alterations change the dynamics of early patterns of activity that are required for proper brain development. Such patterns of activity have been described in both human premature brain (the delta brush) at stages where Kv7.2 channels are expressed,^{12,13} and in rodent brain (spindle burst and early gamma oscillations) during the first postnatal week of life.^{12–14} It has been proposed that these patterns play an important role in the formation of cortical circuits before the onset of any external sensory input.¹³ Of interest, this developmental stage corresponds in rodent to a critical period, where a

dominant negative mutation in *KCNQ2* led to an increase in the rate of spindle burst and later to epilepsy and pathologic behavior.¹⁵

KCNQ2-related EOEEs are resistant to many antiepileptic drugs. M-current increasing compounds (i.e., retigabine, ICA-27243, SF0034, and others) first appeared as promising treatment tools, since most Kv7.2 mutations associated with EOEE reduced Kv7 channel activity.¹ In light of our results and those of others,⁸ these compounds may be inappropriate and may even be more deleterious for patients, while Kv7-channel inhibitors such as linopirdine could bring about a potential benefit. Functional analyses of EOEE mutations are thus critical for selecting therapeutic options. Animal models of EOEE are also needed to unravel how *KCNQ2* mutations affect brain development and to find novel therapeutic alternatives.¹⁵

ACKNOWLEDGMENTS

We thank Drs. Thomas Jentsch and Gisèle Alcaraz for the generous gift of plasmids, antibodies, and critical advice. This work was supported by the Agence National pour la Recherche (ANR-14-CE13-0011-02, EPIK), ERA-Net for Research on Rare Diseases (ANR-13-RARE-0001-01; JD), and the Association Française contre les Myopathies (MNM1 2012-14580; JD). This work was also supported by Institut National de la Santé et de la Recherche Médicale (INSERM), Centre National de la Recherche Scientifique, Programme Hospitalier de Recherche Clinique and Aix-Marseille University.

DISCLOSURE

None of the authors has any conflict of interest to disclose. We confirm that we have read the Journals' position on issues involved in ethical publication and affirm that this report is consistent with those guidelines.

REFERENCES

1. Maljevic S, Lerche H. Potassium channel genes and benign familial neonatal epilepsy. *Prog Brain Res* 2014;213:17–53.
2. Jentsch TJ. Neuronal KCNQ potassium channels: physiology and role in disease. *Nat Rev Neurosci* 2000;1:21–30.
3. Devaux JJ, Kleopa KA, Cooper EC, et al. *KCNQ2* is a nodal K⁺ channel. *J Neurosci* 2004;24:1236–1244.
4. Shah MM, Migliore M, Valencia I, et al. Functional significance of axonal Kv7 channels in hippocampal pyramidal neurons. *Proc Natl Acad Sci USA* 2008;105:7869–7874.
5. Bettefeld A, Tran BT, Gavrilis J, et al. Heteromeric Kv7.2/7.3 channels differentially regulate action potential initiation and conduction in neocortical myelinated axons. *J Neurosci* 2014;34:3719–3732.
6. Orhan G, Bock M, Schepers D, et al. Dominant-negative effects of *KCNQ2* mutations are associated with epileptic encephalopathy. *Ann Neurol* 2014;75:382–394.
7. Abidi A, Devaux J, Molinari F, et al. A recurrent *KCNQ2* pore mutation causing early onset epileptic encephalopathy has a moderate effect on M current but alters subcellular localization of Kv7 channels. *Neurobiol Dis* 2015;80:80–92.
8. Miceli F, Soldovieri MV, Ambrosino P, et al. Early-onset epileptic encephalopathy caused by gain-of-function mutations in the voltage sensor of Kv7.2 and Kv7.3 potassium channel subunits. *J Neurosci* 2015;35:3782–3793.
9. Milh M, Boutry-Kryza N, Suter-Sardo J, et al. Similar early characteristics but variable neurological outcome of patients with

- a de novo mutation of KCNQ2. *Orphanet J Rare Dis* 2013;8:80.
10. Weckhuysen S, Mandelstam S, Suls A, et al. KCNQ2 encephalopathy: emerging phenotype of a neonatal epileptic encephalopathy. *Ann Neurol* 2012;71:15–25.
 11. Weckhuysen S, Ivanovic V, Hendrickx R, et al. Extending the KCNQ2 encephalopathy spectrum: clinical and neuroimaging findings in 17 patients. *Neurology* 2013;81:1697–1703.
 12. Kanaumi T, Takashima S, Iwasaki H, et al. Developmental changes in KCNQ2 and KCNQ3 expression in human brain: possible contribution to the age-dependent etiology of benign familial neonatal convulsions. *Brain Dev* 2008;30:362–369.
 13. Khazipov R, Luhmann HJ. Early patterns of electrical activity in the developing cerebral cortex of humans and rodents. *Trends Neurosci* 2006;29:414–418.
 14. Minlebaev M, Colonnese M, Tsintsadze T, et al. Early γ oscillations synchronize developing thalamus and cortex. *Science* 2011;334:226–229.
 15. Marguet SL, Le-Schulte VT, Merseburg A, et al. Treatment during a vulnerable developmental period rescues a genetic epilepsy. *Nat Med* 2015;21:1436–1444.